Dedicated to innovation in aerospace

NLR-TP-2019-529 | March 2020

Impact response prediction and sensitivity analysis of thick laminated composite plates

CUSTOMER: Royal Netherlands Aerospace Centre

NLR – Royal Netherlands Aerospace Centre

Dedicated to innovation in aerospace

Impact response prediction and sensitivity analysis of thick laminated composite plates

Problem area

Recent developments have enabled the use of composite materials in highly-loaded aerospace structures. For example, composite landing gear components contain sections with 20-100mm thick laminates of 50-200 plies. In general, composite structures are known for their high specific strength properties and, unfortunately, for their low damage tolerance. Especially risks associated to accidental impact damage (e.g., bird impact or hail impact) are critical in designing a damage tolerant composite structure. For thick composite structures, the response to such an impact and the resulting damage can be completely different when compared to thin composite structures. It is therefore important to understand how these structures behave under varying impact conditions.

Description of work

The goal of this report is to study the impact response of thick composite structures and identify the sensitivities to laminate and impactor characteristics. In an earlier report an elastic version of an analytical impact response model has been presented. This model is able to determine the response of a thick laminate to impact in terms of force and displacement histories. In this work, this model is adapted by including elasto-plastic behaviour in the contact formulation. This improved model is validated by comparison with experimental results. Using the analytical impact response model a sensitivity analysis is performed to assess the influence of design variables on the impact response in terms of peak force, impact duration, maximum plate deflection, maximum impactor displacement, and transferred energy. A one-at-a-time sensitivity analysis shows the sensitivity of the impactor and laminate properties, including the layup. A more extensive global sensitivity analysis indicates the effect of fibre and matrix properties. Two 50J impact cases, a small-mass (16.72g) and a large-mass (2274g), on 12, 20, and 40mm thick laminates are studied.

REPORT NUMBER
NLR-TP-2019-529

AUTHOR(S)
N. van Hoorn
C. Kassapoglou
W.M. van den Brink

REPORT CLASSIFICATION
UNCLASSIFIED

DATE
March 2020

KNOWLEDGE AREA(S)
Computational Mechanics and Simulation Technology

DESCRIPTOR(S)
Impact response
Thick composite
Carbon fibre reinforced polymer
Sensitivity analysis

Results and conclusions

The analytical impact response model was compared with impact experiments and despite observed differences proved capable of predicting a wide range of impact events. It became clear from the sensitivity analysis that there are many factors that affect the impact response, making it a complex problem.

The impactor mass mainly contributes to the type of response, that is from a localised response (i.e., thick laminate small-mass), to a complex intermediate-mass response, to a quasi-static response (i.e., thin laminate large-mass). For a small-mass impact, the plate deflection history is delayed compared to the force response whereas these histories align for a large-mass impact. The laminate dimensions have a negligible effect on a localised impact response, with the thickness as an exception. It was confirmed that a localised impact response is unaffected by the plate natural frequencies. The laminate layup only affects a quasi-static response with the highest sensitivities on the plate deflection and the transferred energy. It was concluded that the fibre and matrix properties mainly affect the impact response due to changes in laminate stiffness. In terms of global quasi-static behaviour the laminate stiffness affects the plate deflection and plate natural frequencies, while locally the through-thickness stiffness affects the contact behaviour.

Thick composite structures generally have a localised impact response, whereas thin composite structures tend towards a quasi-static impact response with more bending. The difference in response will have a significant effect on the resulting damage mechanism.

Applicability

This study is part of an on-going research program on the impact damage tolerance of thick composite structures and provides useful information for modelling the complex damage mechanisms. The next step is to develop a numerical model that can predict the impact damage in a thick composite structure. To make this model efficient, the results from the analytical impact response model can be used for simplifications while keeping the same accuracy.

GENERAL NOTE

This report is an updated version of NLR-TP-2017-460 that contains a paper presented at the 6th ECCOMAS Thematic Conference on Mechanical Response of Composites, Eindhoven, 20-22 September 2017.

NLR
Anthony Fokkerweg 2
1059 CM Amsterdam, The Netherlands
p) +31 88 511 3113
e) info@nlr.nl i) www.nlr.nl

Dedicated to innovation in aerospace

NLR-TP-2019-529 | March 2020

Impact response prediction and sensitivity analysis of thick laminated composite plates

CUSTOMER: Royal Netherlands Aerospace Centre

AUTHOR(S):

N. van Hoorn	NLR
C. Kassapoglou	Delft University of Technology
W.M. van den Brink	NLR

NLR – Royal Netherlands Aerospace Centre

This report is an updated version of NLR-TP-2017-460 that contains a paper presented at the 6th ECCOMAS Thematic Conference on Mechanical Response of Composites, Eindhoven, 20-22 September 2017.

This publication has been refereed by the Advisory Committee AEROSPACE VEHICLES.

CUSTOMER	**Royal Netherlands Aerospace Centre**
CONTRACT NUMBER	**-----**
OWNER	**NLR**
DIVISION NLR	**Aerospace Vehicles**
DISTRIBUTION	**Unlimited**
CLASSIFICATION OF TITLE	**UNCLASSIFIED**

APPROVED BY:		**Date**
AUTHOR	N. van Hoorn	04-03-2020
REVIEWER	R.J.C. Creemers	04-03-2020
MANAGING DEPARTMENT	A.A. ten Dam	10-03-2020

Contents

Abbreviations

ACRONYM	DESCRIPTION
CCA	Composite Cylinder Assemblage
FSDT	First-order Shear Deformation Theory
NLR	Royal Netherlands Aerospace Centre
ODE	Ordinary Differential Equation
QI	Quasi-Isotropic
RTM	Resin Transfer Moulding
UD	Uni-Directional

Impact response prediction and sensitivity analysis of thick laminated composite plates

Niels van Hoorn[1,2], Christos Kassapoglou[2], and Wouter van den Brink[1]

Abstract

In this paper the impact response of thick composite structures and its sensitivity to design variables for different thicknesses is examined. A combination of existing contact models was found to give good results for a wide range of input parameters covering small-mass (high-velocity) and large-mass (low-velocity) impact events. The impact response is evaluated in terms of peak force (F_M), impact duration (t_i), maximum plate deflection ($w_{p,M}$), maximum impactor displacement ($w_{i,M}$), and transferred energy (E_t). It is concluded that small-mass impact on thick laminates results in a localised impact response with short impact times, almost no bending, and approximately 76% of the energy transferred to the specimen. A quasi-static impact response is observed with large-mass impact on thinner laminates. While the peak force is similar to a localised response the impact duration and plate deflection double, and the transferred energy is just 43%. This paper shows a complex interaction of multiple design variables with each different degrees of sensitivity on these two types of impact responses.

Keywords

Impact behaviour, Thick section, Fibre-reinforced polymer, Sensitivity analysis

1 Introduction

Fibre reinforced composite materials are increasingly being used in the aerospace industry. For instance, the structural weight of the new Airbus A350 and Boeing 787 is over 50% composites. Recently, these materials have been implemented in highly-loaded aerospace structures, such as lugs and landing gear components, resulting in thick laminates (i.e., 20-50mm or 80-200 layers). Although these composites are known for their high specific mechanical properties, their tolerance to damage can be low. Impact damage inside the composite laminate (e.g., due to tool drops or runway debris) can be complex and therefore difficult to predict. To compensate for these uncertainties, conservative design strategies are used, which increase the weight and cost of the structure. Accurate damage models might be able to quantify the damage tolerance and clarify the damage mechanisms. In turn, these models could aid the design and certification process

[1]Royal Netherlands Aerospace Centre (NLR)
[2]Delft University of Technology (TU Delft)

Corresponding author:
Niels van Hoorn, Royal Netherlands Aerospace Centre, Voorsterweg 31, 8316 PR Marknesse, The Netherlands
Email: niels.van.hoorn@nlr.nl

resulting in lower weight composite structures.

The laminate response to impact directly relates to the resulting damage[1,2]. Analytical models to predict this response are already available for thin laminates[3,4]. For example, the models of Shivakumar *et al.*[5], Olsson[6–9], Christoforou *et al.*[10,11], and more recently Talagani[12], and Esrail and Kassapoglou[13]. Shivakumar *et al.* present an energy-balance model for prediction of the peak force and two spring-mass models for prediction of the force and displacement histories. While relatively accurate, these models are limited to large-mass low-velocity impact. Olsson worked on a model that assumed the plate deflection as modal impulse responses specifically for wave-controlled small-mass impact[6]. Moreover, he proposed a mass criterion (i.e., impactor mass versus plate mass) for impact classifications in terms of small-mass, intermediate-mass, and large-mass impact[7]. Later he proposed a modified version of the Shivakumar *et al.* model for large-mass impact in combination with a delamination criterion[8] and similarly a modified version of his small-mass model[9]. Based on Olsson's work Talagani proposed a method that solves the non-linear differential equations numerically to work for higher eigenfrequencies[12]. In contrast to the previous authors, Christoforou *et al.* proposed a model similar to the approach of Olsson's small-mass model[6] but representing the assumed modal functions by series expansions and thus accounting for the full range of modes[11]. Therefore, this model is applicable for a wide range of impact masses. Beside the semi-analytical approaches a more detailed analysis requires numerical models, which have been successfully employed for low-velocity impact by the research group of Bouvet *et al.*[14–16] and Tan *et al.*[17].

Studies that focus on relatively thick composite structures are limited. Mittal[18] obtained a closed-form impact response solution that includes transverse shear, relevant for thick laminates. However, this solution only applies to small-mass impact on infinite isotropic plates. Sun and Potti[19,20] focussed on high-velocity impact on composite laminates up to 8.6mm thick and proposed a few relatively simple models. Zhou and Davies[21] studied the response of 10 and 25mm thick woven glass fibre laminates by low-velocity drop-tower experiments up to 1500J. Jackson and Poe[22] investigated the time histories of contact force and transverse shear on relatively thick laminates.

Despite the mentioned studies, the impact response of thick composite structures is not completely understood, partly due to the influence of numerous variables. Therefore, the goal is to study the impact response of thick composite structures and identify the sensitivity to design variables for different thicknesses. This study is part of an on-going research program on the impact damage tolerance of thick composite structures and provides useful information for modelling the complex damage mechanisms. Previous versions of this model that included a Hertzian elastic contact formulation have been published[23,24]. In the present work a Sun-Christoforou contact formulation proposed by Talagani[12] is used and combined with the model of Christoforou and Yigit[11]. This model provides the force, indentation, impactor displacement, and plate deflection history depending on the laminate properties and impact characteristics (i.e., mass and velocity). The sensitivity to laminate and impact properties is analysed to determine their influence on the response, which helps understand the impact response and identify the differences between impact on thin and thick composite structures. A global sensitivity analysis is then used to determine the effect of fibre and matrix material properties on the response.

2 Impact Response Prediction

2.1 Contact Formulation

A contact formulation relates the impactor indentation (δ) to the resulting contact force (F). Compared to thin composite plates, impact on thick composite plates results in large indentation and high contact forces due to minimal plate bending. In this case a simple Hertzian contact formulation is not valid for these large indentations[6,12]. A more appropriate contact model for thick composite plates has been proposed by

Talagani[12]. His suggestion is to divide contact formulation into three stages: elastic Hertzian loading[25], elastic-plastic loading as proposed by Yigit and Christoforou[26], and unloading as proposed by Yang and Sun[27]. The relation between the indentation and force is then given by:

$$F(\delta) = \begin{cases} k_\alpha \delta^{3/2} & \text{for } 0 \leq \delta < \delta_y \\ k_y(\delta - \delta_y) + k_\alpha \delta_y^{3/2} & \text{for } \delta_y \leq \delta \leq \delta_m \\ F_m \left(\frac{\delta - \delta_0}{\delta_m - \delta_0} \right)^{5/2} & \text{for } \delta_m < \delta \geq \delta_0 \end{cases} \tag{1}$$

where δ is the difference in impactor displacement (w_i) and centre plate deflection (w_p). For the unloading phase F_m and δ_m are the maximum force and indentation prior to unloading. The critical indentation (δ_y) is a material dependent parameter and in this work assumed equal to the value used by Talagani (i.e., 0.3048mm). This value results from the use of exponent 5/2 in the part three of Equation 1. The permanent indentation after impact has been defined by Yang and Sun[27] as:

$$\delta_0 = \delta_m \left[1 - \left(\frac{\delta_y}{\delta_m} \right)^{2/5} \right] \tag{2}$$

The Hertzian contact stiffness (k_α) and elastic-plastic contact stiffness (k_y) are given by[26]:

$$k_\alpha = \frac{4 E_z \sqrt{R_i}}{3\left(1 - \nu_{rz}\nu_{zr}\right)} \tag{3}$$

and

$$k_y = \frac{3}{2} k_\alpha \sqrt{\delta_y} \tag{4}$$

It is assumed that the impactor stiffness is significantly larger than the laminate stiffness, so that the impactor can be assumed rigid. For a layup that is not transversely isotropic ν_{xz} is not equal to ν_{yz}. Therefore, ν_{rz} is determined by averaging these two out-of-plane Poisson's ratios. In Equation 3 the through-thickness modulus (E_z) and the out-of-plane Poisson's ratios (ν_{rz} and ν_{zr}) are given in Table 2(c). Olsson[6] and Christoforou[11] assume that $E_z \approx E_{22}$ and that $v_{zr} \approx 0$ for UD plies. For UD plies E_{22} is approximately equal to E_{33}, in contrast to woven fabric plies. Table 2(b) and 2(c) show that $E_z = E_{33}$ and ν_{zr} can be determined to be 0.021. Olsson's and Christoforou's assumption is in line with these results considering the materials in Tables 2(b) and 2(c) is a fabric material.

2.2 Analytical Impact Response Model

Christoforou and Yigit[11] assumed that the plate centre deflection (w_p), that satisfies simply-supported boundary conditions, is described by a series expansion with an unknown amplitude (q_{mn}), that is,

$$w_p = \sum_{m=1}^{\infty} \sum_{n=1}^{\infty} q_{mn} s_{mn} \tag{5}$$

where, for centrally loaded plates,

$$s_{mn} = \sin \frac{m\pi}{2} \sin \frac{n\pi}{2}$$

The amount of terms used (i.e., m and n) in Equation 5 defines the accuracy. The substitution of this assumption in the governing equations has already been performed by Christoforou and Swanson [10]. In their contribution they take a specially orthotropic form ($A_{16} = A_{26} = B_{ij} = D_{16} = D_{26} = 0$) of the Whitney and Pagano [28] plate equations of motion derived by Dobyns [29]. Transverse shear stresses are more dominant in thick composites, because there is almost no bending. Therefore, the plate stiffness components D_{ij} and A_{ij} are determined using the First-order Shear Deformation Theory (FSDT). Inserting Equation 5 into these plate equations of motion gives a system of second-order Ordinary Differential Equations (ODEs) as described by:

$$\frac{d^2 q_{mn}}{dt^2} + \omega_{mn}^2 q_{mn} = \frac{4F}{m_p} s_{mn} \tag{6}$$

The natural frequencies (ω_{mn}^2) of a simply supported composite laminate that result from this derivation can be found in the contribution of Christoforou and Swanson [10]. In addition to a description of the plate motion an ODE is required to describe the impactor behaviour. This is obtained by substituting $\delta = w_p - w_i$ and Equation 5 into Newton's Second Law (i.e., $m_i \ddot{w}_i = -F$), resulting in:

$$\sum_{m=1}^{\infty} \sum_{n=1}^{\infty} \left(\frac{d^2 q_{mn}}{dt^2} s_{mn} \right) + \frac{d^2 \delta}{dt^2} = -\frac{F}{m_i} \tag{7}$$

In the above equations m_p and m_i are the plate and impactor mass. The system of $m \times n + 1$ second-order ODEs has to be reduced to the first order by introducing the following set of variables:

$$\begin{aligned} q_{mn,1} &= q_{mn} \\ q_{mn,2} &= q'_{mn} \\ \delta_1 &= \delta \\ \delta_2 &= \delta' \end{aligned} \tag{8}$$

Substituting these variables and the Sun-Christoforou contact model (Equation 1) in Equations 6 and 7 gives a $2 \times m \times n + 2$ system of first-order ODEs:

$$\begin{aligned} q'_{mn,1} &= q_{mn,2} \\ q'_{mn,2} &= \frac{4F(\delta_1)}{m_p} s_{mn} - \omega_{mn}^2 q_{mn,1} \\ \delta'_1 &= \delta_2 \\ \delta'_2 &= -\frac{F(\delta_1)}{m_i} - \sum_{m=1}^{\infty} \sum_{n=1}^{\infty} s_{mn} q'_{mn,2} \end{aligned} \tag{9}$$

It is assumed that initial rate of indentation (δ_2) is equal to the initial impactor velocity ($v_{i,0}$), and the other variables in Equation 8 are zero initially. The system of first-order ODEs in Equation 9 is solved using *ode45* in *Matlab**. As a result the indentation $\delta(t)$ and $q_{mn}(t)$ histories are obtained. The force history $F(t)$ is subsequently determined using Equation 1 and the plate deflection history $w_p(t)$ is recovered from Equation 5. The impactor velocity $v_i(t)$ and displacement $w_i(t)$ histories are calculated by integrating the impactor acceleration.

* *ode45* solves non-stiff differential equations based on a variable step Runge-Kutta method.

Table 1. Comparison of predicted impact response parameters (i.e., peak force F_M, maximum plate deflection $w_{i,M}$, and transferred energy E_t) with experimental results.

h [mm]	$E_{i,avg}$ [J]	F_M [kN] exp	F_M [kN] predicted	$w_{i,M}$ [mm] exp	$w_{i,M}$ [mm] predicted	E_t [%] exp	E_t [%] predicted
Small-mass (16.72g)							
19.9	53.31	33.09	44.56 (+34.7%)	2.82	2.28 (-19.3%)	91.68	72.37 (-21.1%)
19.9	96.71	44.62	59.89 (+34.2%)	3.73	3.04 (-18.4%)	92.97	74.89 (-19.4%)
39.4	55.14	37.09	50.32 (+35.6%)	2.59	2.19 (-15.3%)	92.40	70.46 (-23.7%)
39.4	98.86	51.53	67.40 (+30.8%)	3.36	2.90 (-13.7%)	91.60	73.30 (-20.0%)
Large-mass (2274g)							
19.9	55.40	49.73	47.68 (-4.1%)	2.13	2.42 (+13.7%)	78.03	50.43 (-35.4%)
19.9	100.79	52.59	64.40 (+22.5%)	3.30	3.23 (-2.1%)	82.15	53.05 (-35.4%)
39.4	55.24	53.82	51.78 (-3.8%)	1.98	2.23 (+12.4%)	84.13	60.43 (-28.2%)
39.4	101.32	58.50	70.16 (+19.9%)	3.07	2.98 (-2.7%)	84.43	63.33 (-25.0%)

In Figure 1, the obtained solution is compared to the results obtained by Christoforou and Yigit[11] and Sun and Chen[30]. Despite a different prediction of the second peak due to the different contact formulation there is a good agreement considering the first peak. However, this comparison is for a small-mass (8.537g) low-velocity (3m/s) impact event on a thin laminate (2.69mm). Therefore the impact response model for thick laminates is compared with experiments performed at the Royal Netherlands Aerospace Centre (NLR). Figure 2 shows a comparison with a 55.40J large-mass (2274g) impact on a 19.9mm thick specimen. A more extensive comparison is given in Table 1.

The results in Table 1 are averaged over four near identical impacts on similar specimens. All specimens are 150×100mm and impacted with a 16mm diameter hardened steel spherical impactor. The laminate is manufactured using a quasi-UD 2/2 twill weave fabric with a quasi-isotropic $[45, 90, -45, 0]_{ns}$ layup where $n = 8$ for the 19.9mm thick specimens and $n = 16$ for the 39.4mm thick specimens. The fabric has 24K

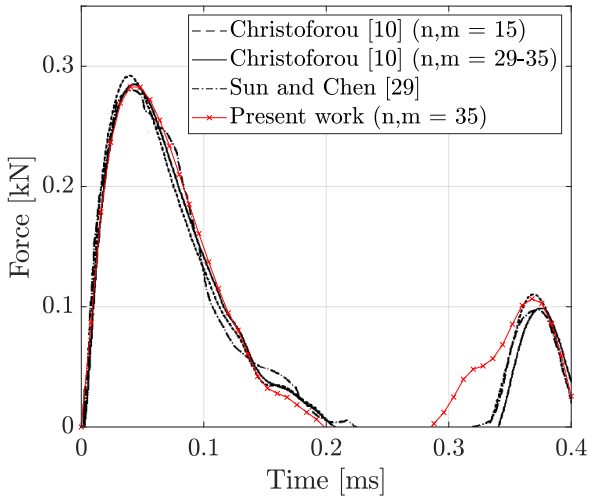

Figure 1. Comparison of the analytical impact response model and solutions from literature[11,30].

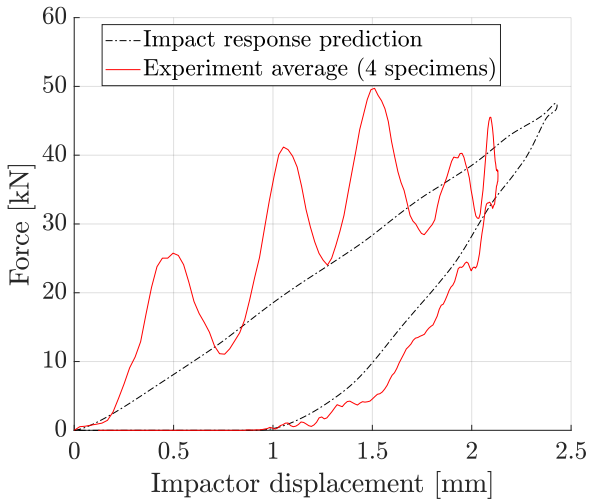

Figure 2. Comparison of the predicted impact response with a 55.40J large-mass (2274g) impact.

Table 2. (a) Fabric and matrix properties, (b) resulting ply properties according to the CCA model, and (c) the derived equivalent laminate membrane properties.

(a)

E_{f11}	275	GPa
E_{f22}	15	GPa
G_{f12}	15	GPa
G_{f23}	7.5	GPa
ν_{f12}	0.2	-
E_m	3	GPa
ν_m	0.35	-
n_{warp}	50	%
V_f	50	%
c_f	0.9	-

(b)

E_{11}	65.97	GPa
E_{22}	65.97	GPa
E_{33}	7.01	GPa
G_{12}	2.75	GPa
G_{13}	2.54	GPa
G_{23}	2.54	GPa
ν_{12}	0.02	-
ν_{13}	0.34	-
ν_{23}	0.34	-
t_{ply}	0.25	mm

(c)

E_x	46.07	GPa
E_y	46.07	GPa
E_z	7.01	GPa
G_{xy}	17.47	GPa
G_{xz}	2.54	GPa
G_{yz}	2.54	GPa
ν_{xy}	0.32	-
ν_{xz}	0.24	-
ν_{yz}	0.24	-
h	4·n	mm

warp and 12K weft yarns with an intermediate modulus carbon fibre. The plates are infused and cured by Resin Transfer Moulding (RTM) with a 180°C cure low viscosity toughened liquid epoxy resin. For the 19.9mm specimens the resulting fibre volume fraction is 59.63% and the laminate density is 1561.97 kg/m^3. For the 39.4mm specimens the resulting fibre volume fraction is 60.23% and the laminate density is 1565.24 kg/m^3. The Hertzian contact stiffness (i.e., Equation 3) for these specimens is 10.91×10^8N/m$^{1.5}$.

From Table 1 it can be observed that there is relatively good agreement for the large-mass drop-tower experiments. In the case the peak force is predicted quite accurately the predicted maximum impactor displacement is about 13-14% higher and vice versa. Comparison with the small-mass impact gun experiments shows a 31-35% difference in predicted force and 14-19% difference in impactor displacement. These differences can be explained by three aspects. One, damage is not explicitly accounted for in the impact response model. Secondly, the impact response model assumes simply-supported boundary conditions while in the experiment the specimen is closer to clamped. In addition, for the small-mass impact gun experiments the impactor displacement and force histories are derived from high speed images. The transferred energy in terms of a percentage with respect to the impact energy is determined using:

$$E_t = \left(1 - \frac{v_{i,e}^2}{v_{i,0}^2}\right) \times 100 \tag{10}$$

where $v_{i,e}$ is the exit/rebound impactor velocity. For all impact tests the predicted transferred energy is about 19-24% lower for small-mass impact and 25-35% lower for large-mass impact. Despite these differences the model is considered applicable for deriving the impact response sensitivities.

3 Sensitivity Analysis

In this section an extensive sensitivity analysis is performed where the effect of relevant input parameters on the impact response is assessed. The following output parameters are evaluated: peak force (F_M), impact duration[†] (t_i), maximum plate deflection ($w_{p,M}$), maximum impactor displacement ($w_{i,M}$), and transferred energy (E_t). The detailed sensitivity analysis results are given in Appendix A.

[†]The impact duration is measured from $t = 0$ to the point the impactor reaches its start position at $t = 0$.

3.1 Material Properties

The fibre and matrix properties used for the sensitivity analysis in Table 2(a) are partly based on the work of Soden *et al.*[31]. From these properties, the ply properties of a single Uni-Directional (UD) layer are derived using Hashin's Composite Cylinder Assemblage (CCA) model[32]. It is assumed that the fabric is represented by two stacked UD plies, one ply oriented 0° and another ply oriented 90°. By weighing these two plies depending on de percentage of yarns in warp direction (n_{warp}) the fabric ply properties are derived. In addition, a correction factor (c_f) degrades the fibre properties to account for fibre undulations. The above results in the ply properties in Table 2(b), where the 1-direction aligns with the warp yarns and 2-direction with the weft yarns. An anti-symmetric balanced Quasi-Isotropic (QI) layup is used:

$$[-45, 45, 0, 90, 45, -45, 90, 0, 0, 90, 45, -45, 90, 0, -45, 45]_n$$

which is chosen in order to comply with the assumptions in the governing equations. For this layup, the B-matrix, the shearing-stretching coupling terms (A_{16}, A_{26}), and bending-twisting coupling terms (D_{16}, D_{26}) are zero. The integer n defines the thickness (h), for example $h = n_{ply} \cdot t_{ply} \cdot n$, where $n_{ply} = 16$ and $t_{ply} = 0.25$mm. The equivalent laminate membrane properties in Table 2(c) are derived from the laminate stiffness tensor (see Appendix B), with x and y the in-plane laminate coordinates. The procedure above allows the use of arbitrary fibre and matrix properties (see Section 3.4) and obtains the resulting three-dimensional laminate properties without the need of experimentally obtained values.

The following reference properties are established for the sensitivity analysis. A rigid spherical impactor with a radius (R_i) of 10mm is used for impact on a 200×200mm simply-supported 20mm thick (i.e., $n = 5$) plate. Two 50J impact cases are considered; a small-mass 16.72g ($v_{i,0}$ = 77.34m/s) impact case (e.g., runway debris), and a large-mass 2274g ($v_{i,0}$ = 6.63m/s) impact case (e.g., tool drop).

3.2 Sensitivity to the Impactor and Laminate Properties

First, a local sensitivity analysis is performed to determine the sensitivity of the impactor and laminate properties, see Table 3. Each case evaluates a small-mass and large-mass impact event, except for the impactor mass sensitivity. Detailed results regarding the impactor mass sensitivity are given in Table 4 and the sensitivity of other properties in Table 5.

The sensitivity to the impactor mass is high and it can significantly change the impact response. For instance, the impact duration increases from 0.120, to 0.448, and 1.372ms. Figure 3 shows the difference between the three types of impact (i.e., small-mass, intermediate-mass, and large-mass impact) by plotting the force and plate deflection versus time. In contrast to large-mass impact, the plate deflection is delayed compared to the force for small-mass impact. For the intermediate-mass impact, there is still a small delay of the plate deflection. In addition, the force history is complex, as it can have more than one peak, representing

Table 3. Input to the local sensitivity analysis of the impactor and laminate properties. The parameters that determine the response are varied one-at-a-time compared to the reference values in bold.

Variable	Units	Values					
Impactor mass (m_i)	mm	**16.72**	-	140	-	**2274**	(constant E_i)
Impactor energy (E_i)	J	**50**	-	100	-	150	(constant m_i)
Impactor radius (R_i)	mm	5	-	**10**	-	15	
Laminate thickness (h)	mm	12	-	**20**	-	40	
Laminate width,height (a, b)	mm	100	-	**200**	-	300	
Laminate aspect ratio (AR)		**1**	-	2	-	3	(constant area)

multiple impacts. From now on, impacts are categorised as a localised impact response (i.e., small-mass impact on a thick laminate) and a quasi-static impact response (i.e., large-mass impact on a thin laminate). Table 4 also shows that for a quasi-static impact response significantly less (i.e., 43%) kinetic energy is transferred from the impactor to the specimen compared to 76% for a localised impact response. Neglecting possible temperature increases and sound waves, this transferred energy is dispersed as damage dissipation energy and elastic (stored) energy (i.e., bending). For a quasi-static impact response part of this bending energy is recouped as impactor kinetic energy. For a localised impact response, this is not possible due to the delayed plate deflection. Interestingly, the transferred energy for intermediate-mass impacts is even higher which could imply that a larger percentage of the energy is dissipated by damage creation.

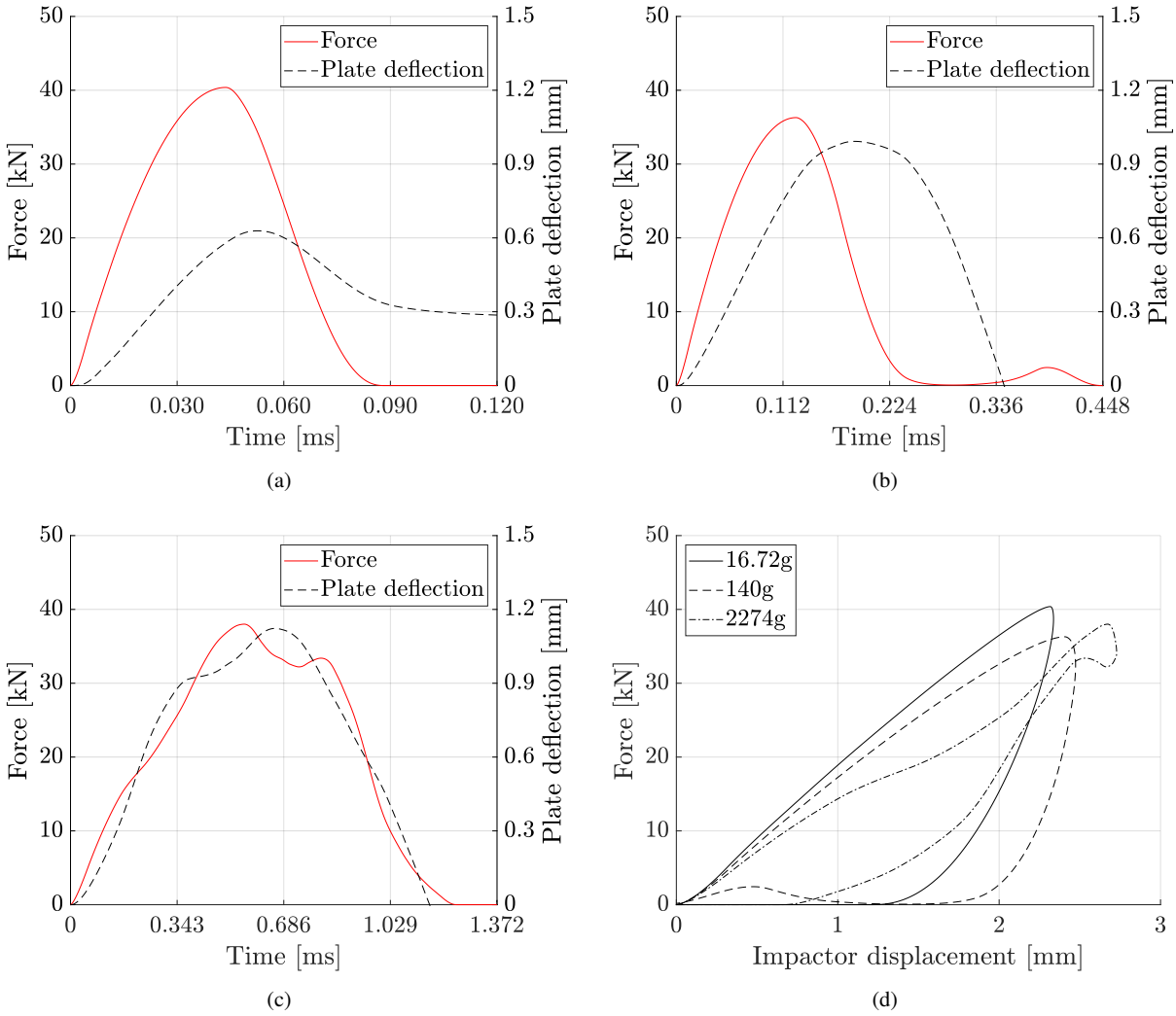

Figure 3. Force and plate deflection histories illustrating the sensitivity to the impactor mass for a 50J (a) small-mass (16.72g), (b) intermediate-mass (140g), and (c) large-mass (2274g) impact. In (d) the sensitivity is visualised using force versus impactor displacement.

For a constant impactor mass, the response sensitivity to the impactor energy is low because the force and displacements are increased almost exactly in proportion to the impactor velocity (i.e. $\sqrt{2}$ and $\sqrt{3}$ for 100J and 150J respectively). At the same time the impact duration is only slightly increased for a localised impact response. This is expected, as the impactor velocity is an initial condition and can be seen as the amplitude of the system of differential equations. Though increasing, the peak force is expected to plateau at high energy levels, as concluded by Zhou and Davies[21]. The sensitivity to the impactor radius has no significant effect on the response shape, but increasing the impactor radius increases the force and decreases the impactor displacement. This effect is identical to scaling the contact stiffness.

The response has a high sensitivity to the laminate dimensions, for instance the thickness (Figure 5), the area, and the aspect ratio. Increasing the thickness as well as the area doubles the laminate mass and according to Olsson the impactor/plate mass ratio dictates the response[7]. Olsson stated that a ratio below 0.23 can be considered small-mass and above 2.0 large-mass impact. However, the results indicate that the laminate bending stiffness also plays a significant role. For example, increasing the thickness or decreasing the area results in a higher bending stiffness. From Figure 5 it is observed that thicker laminates tend more to a localised response. For thicker laminates, more energy is absorbed into indentation during the loading phase, instead of bending energy. According to the model of Esrail and Kassapoglou[13], for a thickness of 12mm about 88% of the energy converts to bending energy compared to 17% for a 40mm thick laminate. Thus for thick laminates the plate deflection can be neglected, as was concluded by Zhou and Davies[21]. While the indentation energy directly results in damage the creation of delaminations and transverse cracks result from the interaction of indentation, bending, and stress waves.

Varying the plate dimensions (e.g., area a, b and aspect ratio AR) only affect the plate mass m_p and natural frequencies ω^2_{mn} in the differential equations in Equation 9. A characteristic of a localised response is that it is insensitive to the plate natural frequencies. This is confirmed by the effect of aspect ratio (see Table 5) where the plate area (i.e., mass) is kept constant. In contrast to a quasi-static impact response, increasing the laminate area has a negligible effect on a localised impact response.

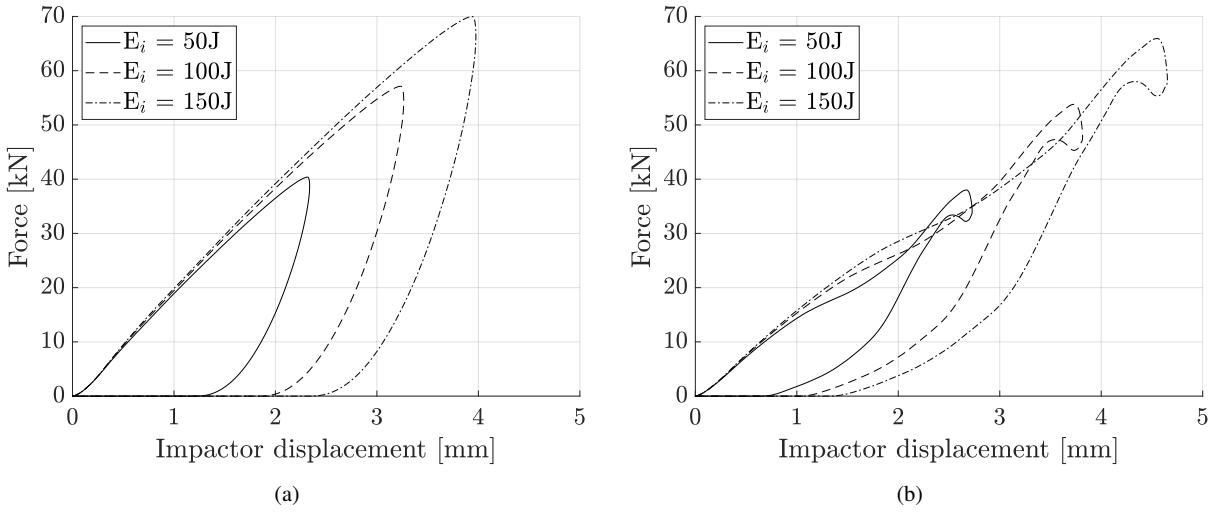

Figure 4. Force versus impactor displacement illustrating the sensitivity to the impactor energy for (a) small-mass and (b) large-mass impact.

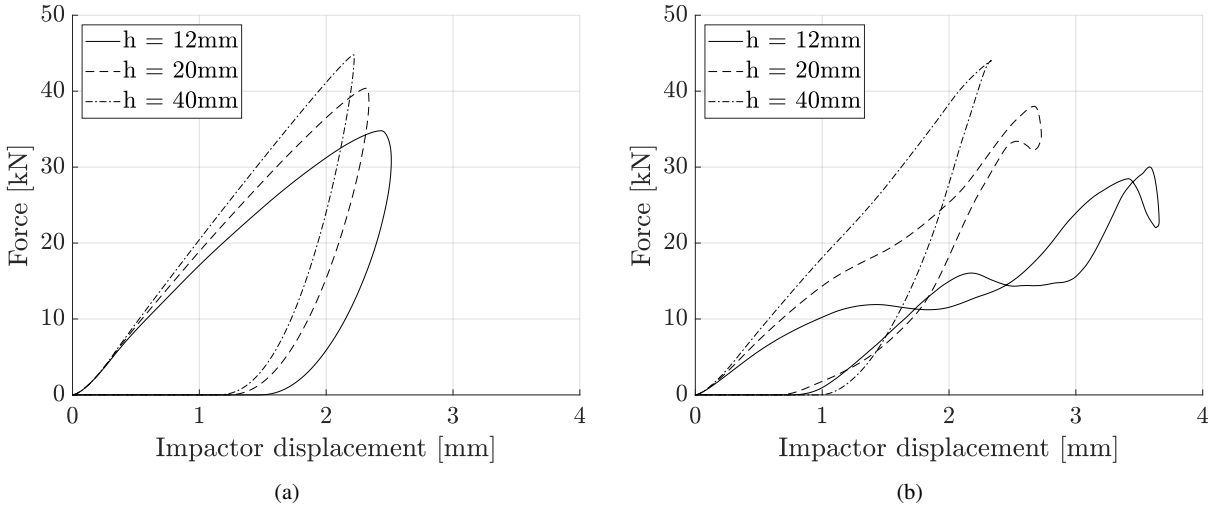

Figure 5. Force versus impactor displacement illustrating the sensitivity to the laminate thickness for (a) small-mass and (b) large-mass impact.

3.3 Sensitivity to the Laminate Layup

Changing the laminate layup changes the properties of the laminate and is therefore expected to change the response. To study this effect, a $0°$ and $\pm 45°$ only layup are evaluated in addition to the Quasi-Isotropic (QI) layup given in Section 3.1 for a 12, 20, and 40mm thick laminate. It is concluded that changing the layup has a negligible effect on a localised impact response (i.e., $<1\%$), which agrees with the observations from Section 3.2. A quasi-static impact response is more sensitive to the layup change, see Table 6. In this case, increasing the number of $0°$ layers results in a significantly larger plate deflection and thus less transferred energy. The $\pm 45°$ is more efficient in absorbing impact energy as indicated by the lower peak force and impact duration. For thick plates the impact response is almost insensitive to the layup with the plate deflection as an exception. Note that in Table 6 the peak force and impact duration of the QI laminate correspond to Figure 5(b).

3.4 Sensitivity to the Material Properties

In the previous sections a local one-at-a-time sensitivity analysis gave insight in the sensitivity of the impactor and laminate properties. This section presents a more extensive global sensitivity analysis on the fibre and matrix material properties. For this analysis an open source Python library *SALib* is used. The lower and upper bounds of the input parameters are defined as 80% and 120% of the values in Table 2(a). A priori it was determined that the fibre in-plane Poisson's ratio (ν_{f12}) and shear modulus (G_{f12}) have a negligible effect on the impact response. In addition, the percentage of yarns in warp direction (n_{warp}) has no effect because a QI layup is evaluated, leaving six input parameters (D) to evaluate. Saltelli sampling sequence[33], a quasi Monte Carlo sampling technique, within SALib generates the inputs. The interval per parameter (N) is set to 2,000, resulting in a $[2N(D+1) \times D] = [28,000 \times 6]$ input matrix. $N = 2,000$ gives a reasonable range of confidence.

The analytical impact response model evaluates these 28,000 inputs and for each case the impact characteristics are stored. The effect the input parameters have on these characteristics is analysed using the

Sobol method within SALib[34]. As a result the sensitivities are expressed in Sobol indices within a certain range of confidence. The first-order indices (S_i), or main effect indices, give the effect of parameter i only. Note that $\sum_{i=1}^{D} S_i = 1$. Higher-order indices (i.e., S_{ij}) give the effect of multiple parameters on the output. However, the number of parameters is quite large and as a result it is difficult to evaluate the effect of all interactions. Therefore, the total-effect index (S_{Ti}) is given which includes the variance of all interactions. For almost all input parameters the total-order sensitivity index is close to the first-order sensitivity index, indicating almost no higher-order interactions. Therefore, the total-order is not shown in the results in Figure 6 and 7.

An overview of the first-order sensitivities is given in Table 7 and the sensitivities on two impact response characteristics are given in Figure 6 and 7. In general it is observed that the sensitivities on the peak force (F_M), impact duration (t_i), and maximum impactor displacement ($w_{i,M}$) are showing similar trends. In contrast to these three impact characteristics, the sensitivities on the maximum plate deflection ($w_{p,M}$) and transferred energy (E_t) are different.

While the fibre longitudinal modulus (E_{f11}) is a main contributor to the laminate stiffness, it has a negligible effect on the peak force for a localised impact response (see Figure 6(a)). Only a quasi-static impact response is sensitive to E_{f11} because it affects the bending behaviour of the plate. Interestingly, the transferred energy for a localised impact response is highly sensitive to E_{f11}, see Figure 7(a). There is no clear physical explanation, other than that the sensitivity of other parameters on the transferred energy is even smaller. The fibre transverse modulus (E_{f22}) shows an inverse trend compared to E_{f11} and the sensitivity increases for thicker laminates. This is due to the fact that E_{f22} contributes significantly to the through-thickness stiffness of the laminate. The impact response is moderately sensitive to the fibre out-of-plane shear modulus (G_{f23}), but interestingly increasing this value decreases the peak force and thus could increase the impact damage tolerance, especially for thick laminates.

In terms of matrix properties the peak force is quite sensitive to the matrix modulus (E_m). On the other hand, it has almost no effect on the maximum plate deflection and transferred energy for large-mass impact. An explanation is that for a twice as large E_m, the through-thickness modulus (E_{33}) increases by 47%, while

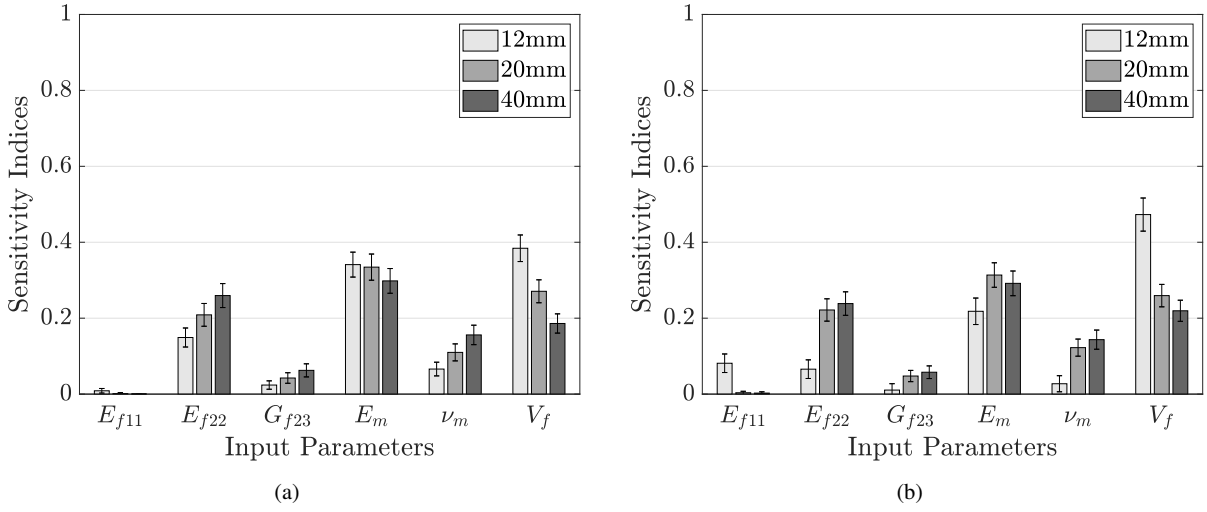

Figure 6. First-order Sobol indices indicating the sensitivity of the material properties on the peak force for (a) small-mass and (b) large-mass impact on 12, 20, and 40mm thick laminates.

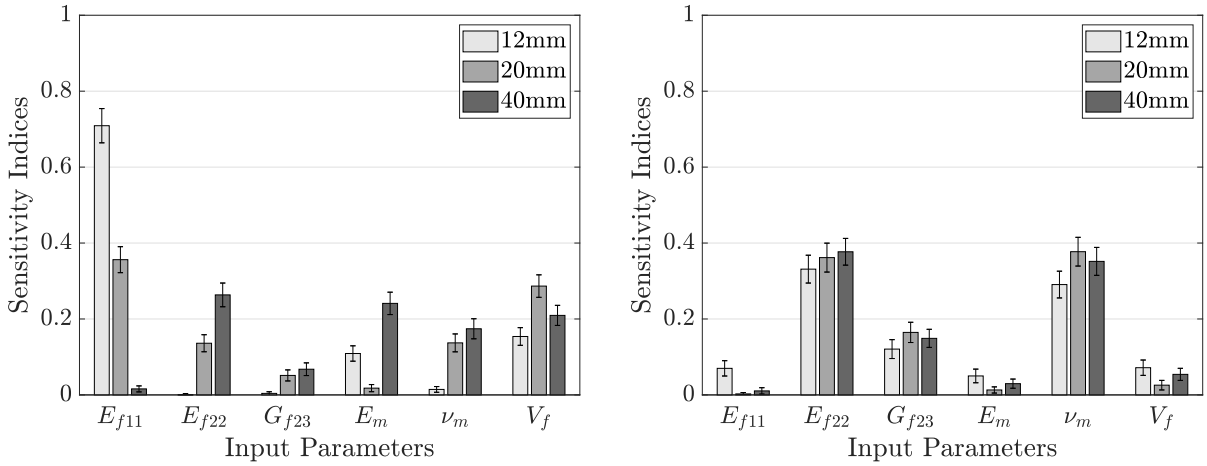

Figure 7. First-order Sobol indices indicating the sensitivity of the material properties on the transferred energy for (a) small-mass and (b) large-mass impact on 12, 20, and 40mm thick laminates.

the in-plane stiffness ($E_{11/22}$) only increase by 4%. As a result, the effect on plate deflection is negligible and the increase of E_m only affects the indentation resulting in a higher peak force. For a more localised impact response, that involves mainly E_{33}, the sensitivity of E_m on the plate deflection and transferred energy is larger. While the matrix Poisson's ratio (ν_m) has a moderate effect on most impact characteristics, it has a significant effect on the transferred energy for a quasi-static impact response.

The impact response is highly sensitive to the fibre volume faction (V_f), with the maximum plate deflection in particular, specially for a quasi-static impact response. This is due to the fact that V_f is the main contributor to the laminate stiffness. While the fibre moduli (E_{f11} and E_{f22}) have a similar influence on the laminate in-plane stiffness, the effect on the impact response differs because the effect on through-thickness stiffness is dissimilar.

4 Summary and Conclusions

This paper has studied the impact response of thick composite structures and identified the sensitivities of several design variables on the impact response. The proposed analytical impact response model combines the impact response model of Christoforou and Yigit[11] with the Sun-Christoforou contact formulation suggested by Talagani[12]. The analytical impact response model was compared with impact experiments and despite observed differences proved capable of predicting a wide range of impact events. Using the analytical impact response model an extensive sensitivity analysis was performed to assess the influence of design variables on the impact response in terms of peak force (F_M), impact duration (t_i), maximum plate deflection ($w_{p,M}$), maximum impactor displacement ($w_{i,M}$), and transferred energy (E_t). A one-at-a-time sensitivity analysis showed the sensitivity of the impactor and laminate properties, including the layup. A more extensive global sensitivity analysis indicated the effect of fibre and matrix properties. Two 50J impact cases, a small-mass (16.72g) and a large-mass (2274g), on 12, 20, and 40mm thick laminates were studied. It is clear that there are many factors that affect the impact response, making it a complex problem. From the results in Section 3 the following conclusions can be drawn in terms of sensitivity:

The impactor mass mainly contributes to the type of response, that is from a localised response (i.e., thick laminate small-mass), to a complex intermediate-mass response, to a quasi-static response (i.e., thin laminate large-mass). For a small-mass impact, the plate deflection history is delayed compared to the force response whereas these histories align for a large-mass impact. The laminate dimensions have a negligible effect on a localised impact response, with the thickness as an exception. It was confirmed that a localised impact response is unaffected by the plate natural frequencies. Thicker laminates (i.e., small a/h ratio) have a higher bending stiffness. As a result, the impact energy is mainly converted to indentation instead of bending. According to the sensitivities shown in Section 3.1 a simple mass criterion, as proposed by Olsson[7], may not be sufficient to classify the type of impact response. The laminate layup only affects a quasi-static response with the highest sensitivities on the plate deflection and the transferred energy. In Section 3.3 it was concluded that the fibre and matrix properties mainly affect the impact response due to changes in laminate stiffness. In terms of global quasi-static behaviour the laminate stiffness affects the plate deflection and plate natural frequencies, while locally the through-thickness stiffness (E_{33}) affects the contact behaviour. For instance, the fibre longitudinal modulus (E_{f11}) shows a high sensitivity in the case of a quasi-static impact response. On the other hand, the fibre transverse modulus (E_{f22}) and matrix modulus (E_m) have a higher sensitivity for a localised impact response. The impact response is highly sensitive to the fibre volume fraction, especially for a quasi-static impact response, because it is the main contributor to the laminate stiffness.

The response of thick composite structures to impact can be completely different from the impact response of thin composite structures. In the end, the energy that goes into bending and indentation will result in damage. Thick composite structures generally have a localised impact response, whereas thin composite structures tend towards a quasi-static impact response with more bending. The difference in response will have a significant effect on the resulting damage mechanism.

A Detailed Sensitivity Analysis Results

In this section the detailed results of the sensitivity analysis are given. The impact response is evaluated in terms of peak force (F_M), impact duration (t_i), maximum plate deflection ($w_{p,M}$), maximum impactor displacement ($w_{i,M}$), and transferred energy (E_t). The results of Section 3.2 are given in Tables 4 and 5. Table 6 shows the layup sensitivity and the results of the global sensitivity analysis of the fibre and matrix properties are given in Table 7.

Table 4. Impact response sensitivity to the impactor mass corresponding to Figure 3.

m_i [g]	F_M [kN]	t_i [ms]	$w_{p,M}$ [mm]	$w_{i,M}$ [mm]	E_t [%]
16.72	40.38	0.12	0.63	2.34	75.90
140	36.29	0.45	0.99	2.47	84.85
2274	38.00	1.37	1.12	2.73	42.64

Table 5. Impact response sensitivity to the impactor and laminate properties. The percentage differences are with respect to the reference properties which concern a 50J impact with a 10mm radius impactor on a 20mm thick 200×200mm specimen.

		F_M [kN]	t_i [ms]	$w_{p,M}$ [mm]	$w_{i,M}$ [mm]	E_t [%]
		Small-mass (16.72g)				
Reference		40.38	0.12	0.63	2.34	75.90
E_i	100J	57.13 (+41.5%)	0.12 (+1.5%)	0.89 (+40.9%)	3.26 (+39.7%)	78.46 (+3.4%)
	150J	69.98 (+73.3%)	0.12 (+2.6%)	1.08 (+72.1%)	3.98 (+70.1%)	79.77 (+5.1%)
R_i	5mm	35.57 (-11.9%)	0.14 (+15.9%)	0.59 (-6.9%)	2.70 (+15.4%)	76.88 (+1.3%)
	15mm	43.25 (+7.1%)	0.11 (-7.8%)	0.65 (+4.0%)	2.16 (-7.7%)	75.42 (-0.6%)
h	12mm	34.79 (-13.8%)	0.14 (+19.1%)	1.06 (+68.8%)	2.51 (+7.6%)	82.88 (+9.2%)
	40mm	44.79 (+10.9%)	0.11 (-8.7%)	0.32 (-49.2%)	2.22 (-5.0%)	72.92 (-3.9%)
a, b	100mm	39.46 (-2.3%)	0.12 (+0.8%)	0.72 (+14.4%)	2.40 (+2.6%)	74.16 (-2.3%)
	300mm	40.93 (+1.4%)	0.12 (+0.3%)	0.58 (-7.9%)	2.30 (-1.6%)	77.64 (+2.3%)
AR	2	40.48 (+0.2%)	0.12 (+0.1%)	0.62 (-1.4%)	2.33 (-0.3%)	76.30 (+0.5%)
	3	40.61 (+0.6%)	0.12 (+0.4%)	0.61 (-3.3%)	2.32 (-0.7%)	76.95 (+1.4%)
		Large-mass (2274g)				
Reference		38.00	1.37	1.12	2.73	42.64
E_i	100J	53.81 (+41.6%)	1.37 (-0.1%)	1.58 (+41.0%)	3.82 (+39.9%)	45.27 (+6.2%)
	150J	65.93 (+73.5%)	1.37 (-0.1%)	1.94 (+72.3%)	4.65 (+70.5%)	46.63 (+9.4%)
R_i	5mm	33.13 (-12.8%)	1.53 (+11.5%)	1.05 (-6.8%)	3.03 (+11.2%)	46.21 (+8.4%)
	15mm	40.76 (+7.3%)	1.29 (-5.8%)	1.17 (+4.3%)	2.58 (-5.4%)	39.89 (-6.5%)
h	12mm	30.01 (-21.0%)	1.80 (+31.1%)	2.46 (+119.2%)	3.66 (+34.0%)	23.12 (-45.8%)
	40mm	44.01 (+15.8%)	1.21 (-11.9%)	0.45 (-60.0%)	2.33 (-14.4%)	56.24 (+31.9%)
a, b	100mm	41.08 (+8.1%)	1.28 (-6.6%)	0.79 (-29.8%)	2.54 (-6.9%)	48.30 (+13.3%)
	300mm	34.85 (-8.3%)	1.53 (+11.5%)	1.73 (+53.7%)	2.97 (+8.8%)	44.81 (+5.1%)
AR	2	38.07 (+0.2%)	1.31 (-4.5%)	1.00 (-10.7%)	2.64 (-3.3%)	41.35 (-3.0%)
	3	41.08 (+8.1%)	1.30 (-5.5%)	0.83 (-26.1%)	2.56 (-6.2%)	48.54 (+13.8%)

Table 6. Impact response sensitivity to the laminate layup for 12, 20, and 40mm thick 200×200mm specimens subjected to a 50J large-mass (2274g) impact with a 10mm radius impactor. The percentage differences are defined with respect to the QI layup mentioned in Section 2.

Layup	F_M [kN]	t_i [ms]	$w_{p,M}$ [mm]	$w_{i,M}$ [mm]	E_t [%]
	h = 12mm				
QI	30.01	1.80	2.46	3.66	23.12
±45°	29.62 (-1.3%)	1.72 (-4.7%)	2.37 (-3.7%)	3.50 (-4.2%)	24.12 (+4.3%)
0°	27.82 (-7.3%)	1.94 (+8.0%)	3.03 (+23.1%)	3.93 (+7.6%)	21.47 (-7.1%)
	h = 20mm				
QI	38.00	1.37	1.12	2.73	42.64
±45°	37.80 (-0.5%)	1.34 (-2.1%)	1.07 (-4.8%)	2.69 (-1.4%)	41.76 (-2.1%)
0°	37.69 (-0.8%)	1.42 (+3.7%)	1.24 (+10.4%)	2.81 (+3.2%)	42.70 (+0.1%)
	h = 40mm				
QI	44.01	1.21	0.45	2.33	56.24
±45°	44.25 (+0.5%)	1.21 (+0.4%)	0.43 (-4.2%)	2.33 (+0.0%)	57.24 (+1.8%)
0°	43.86 (-0.3%)	1.21 (+0.4%)	0.48 (+6.2%)	2.34 (+0.4%)	55.71 (-1.0%)

Table 7. Impact response sensitivity to the material properties for 12, 20, and 40mm thick 200×200mm specimens subjected to a 50J impact with a 10mm radius impactor. The sensitivities are quantified as first-order Sobol indices ranging from no sensitivity (0) to high sensitivity (1).

	Small-mass (16.72g)					**Large-mass (2274g)**				
	F_M	t_i	$w_{p,M}$	$w_{i,M}$	E_t	F_M	t_i	$w_{p,M}$	$w_{i,M}$	E_t
12mm										
E_{f11}	0.01	0.04	0.03	0.00	0.71	0.08	0.18	0.27	0.17	0.07
E_{f22}	0.15	0.19	0.01	0.22	0.00	0.07	0.06	0.03	0.06	0.33
G_{f23}	0.02	0.04	0.02	0.05	0.00	0.01	0.01	0.02	0.01	0.12
E_m	0.34	0.25	0.23	0.33	0.11	0.22	0.14	0.02	0.15	0.05
ν_m	0.07	0.11	0.04	0.13	0.01	0.03	0.03	0.04	0.03	0.29
V_f	0.38	0.34	0.66	0.24	0.15	0.47	0.55	0.55	0.56	0.07
20mm										
E_{f11}	0.00	0.00	0.01	0.00	0.36	0.00	0.04	0.13	0.03	0.00
E_{f22}	0.21	0.24	0.02	0.26	0.14	0.22	0.17	0.03	0.16	0.36
G_{f23}	0.04	0.06	0.04	0.06	0.05	0.05	0.04	0.03	0.03	0.16
E_m	0.33	0.29	0.24	0.31	0.02	0.31	0.26	0.08	0.28	0.01
ν_m	0.11	0.15	0.08	0.16	0.14	0.12	0.10	0.06	0.09	0.38
V_f	0.27	0.22	0.60	0.18	0.29	0.26	0.36	0.65	0.37	0.03
40mm										
E_{f11}	0.00	0.00	0.00	0.00	0.02	0.00	0.00	0.03	0.00	0.01
E_{f22}	0.26	0.27	0.04	0.28	0.26	0.24	0.29	0.07	0.25	0.38
G_{f23}	0.06	0.07	0.05	0.07	0.07	0.06	0.07	0.06	0.06	0.15
E_m	0.30	0.29	0.23	0.28	0.24	0.29	0.28	0.12	0.30	0.03
ν_m	0.16	0.18	0.11	0.19	0.17	0.14	0.19	0.13	0.15	0.35
V_f	0.19	0.16	0.54	0.15	0.21	0.22	0.15	0.57	0.20	0.05

B Equivalent Laminate Membrane Properties

The compliance tensor, that relates the stresses to the strains, for an orthotropic laminate[35] is defined as:

$$\begin{Bmatrix} \varepsilon_x \\ \varepsilon_y \\ \varepsilon_z \\ \gamma_{yz} \\ \gamma_{xz} \\ \gamma_{xy} \end{Bmatrix} = \begin{bmatrix} S_{11} & S_{12} & S_{13} & 0 & 0 & S_{16} \\ S_{12} & S_{22} & S_{23} & 0 & 0 & S_{26} \\ S_{13} & S_{23} & S_{33} & 0 & 0 & S_{36} \\ 0 & 0 & 0 & S_{44} & S_{45} & 0 \\ 0 & 0 & 0 & S_{45} & S_{55} & 0 \\ S_{16} & S_{26} & S_{36} & 0 & 0 & S_{66} \end{bmatrix} \begin{Bmatrix} \sigma_x \\ \sigma_y \\ \sigma_z \\ \tau_{yz} \\ \tau_{xz} \\ \tau_{xy} \end{Bmatrix} \tag{11}$$

For each ply k that is at an angle θ the values for S_{ij}^k can be determined by transforming the ply properties (i.e., Table 2(b)) to the laminate coordinate system by using:

$$\begin{aligned}
S_{11}^k &= \frac{1}{E_{11}}\cos^4\theta + \left(\frac{1}{G_{12}} - \frac{2\nu_{12}}{E_{11}}\right)\sin^2\theta\cos^2\theta + \frac{1}{E_{22}}\sin^4\theta \\
S_{12}^k &= \left(\frac{1}{E_{11}} + \frac{1}{E_{22}} - \frac{1}{G_{12}}\right)\sin^2\theta\cos^2\theta - \frac{\nu_{12}}{E_{11}}\left(\sin^4\theta + \cos^4\theta\right) \\
S_{13}^k &= -\frac{\nu_{13}}{E_{11}}\cos^2\theta - \frac{\nu_{23}}{E_{22}}\sin^2\theta \\
S_{22}^k &= \frac{1}{E_{11}}\sin^4\theta + \left(\frac{1}{G_{12}} - \frac{2\nu_{12}}{E_{11}}\right)\sin^2\theta\cos^2\theta + \frac{1}{E_{22}}\cos^4\theta \\
S_{23}^k &= -\frac{\nu_{13}}{E_{11}}\sin^2\theta - \frac{\nu_{23}}{E_{22}}\cos^2\theta S_{33}^k = \frac{1}{E_{33}} \\
S_{16}^k &= \frac{2}{E_{11}}\cos^3\theta\sin\theta - \frac{2}{E_{22}}\cos\theta\sin^3\theta + \left(\frac{1}{G_{12}} - \frac{2\nu_{12}}{E_{11}}\right)\left(\cos\theta\sin^3\theta - \cos^3\theta\sin\theta\right) \\
S_{26}^k &= \frac{2}{E_{11}}\cos\theta\sin^3\theta - \frac{2}{E_{22}}\cos^3\theta\sin\theta + \left(\frac{1}{G_{12}} - \frac{2\nu_{12}}{E_{11}}\right)\left(\cos^3\theta\sin\theta - \cos\theta\sin^3\theta\right) \\
S_{36}^k &= 2\left(\frac{\nu_{23}}{E_{22}} - \frac{\nu_{13}}{E_{11}}\right)\cos\theta\sin\theta \\
S_{44}^k &= \frac{1}{G_{13}}\sin^2\theta + \frac{1}{G_{23}}\cos^2\theta \\
S_{45}^k &= \left(\frac{1}{G_{13}} - \frac{1}{G_{23}}\right)\sin\theta\cos\theta \\
S_{55}^k &= \frac{1}{G_{13}}\cos^2\theta + \frac{1}{G_{23}}\sin^2\theta \\
S_{66}^k &= 4\left(\frac{1}{E_{11}} + \frac{1}{E_{22}} + \frac{2\nu_{12}}{E_{11}}\right)\sin^2\theta\cos^2\theta + \frac{1}{G_{12}}\left(\sin^4\theta + \cos^4\theta - 2\sin^2\theta\cos^2\theta\right)
\end{aligned}$$

The inverse of the ply compliance tensor gives the ply stiffness tensor, for instance $\boldsymbol{C^k} = \left(\boldsymbol{S^k}\right)^{-1}$. With the equal strain assumption, the laminate stiffness tensor can be obtained by averaging the components of all the plies,

$$C_{ij} = \frac{1}{h}\sum_{k=1}^{n} C_{ij}^k t_k \tag{12}$$

where t_k is the thickness of ply k and h the laminate thickness.

$$\begin{Bmatrix} \sigma_x \\ \sigma_y \\ \sigma_z \\ \tau_{yz} \\ \tau_{xz} \\ \tau_{xy} \end{Bmatrix} = \begin{bmatrix} C_{11} & C_{12} & C_{13} & 0 & 0 & C_{16} \\ C_{12} & C_{22} & C_{23} & 0 & 0 & C_{26} \\ C_{13} & C_{23} & C_{33} & 0 & 0 & C_{36} \\ 0 & 0 & 0 & C_{44} & C_{45} & 0 \\ 0 & 0 & 0 & C_{45} & C_{55} & 0 \\ C_{16} & C_{26} & C_{36} & 0 & 0 & C_{66} \end{bmatrix} \begin{Bmatrix} \varepsilon_x \\ \varepsilon_y \\ \varepsilon_z \\ \gamma_{yz} \\ \gamma_{xz} \\ \gamma_{xy} \end{Bmatrix} \tag{13}$$

From the stiffness tensor of the full laminate in Equation 13 the equivalent laminate properties (i.e., E_x, E_y, E_z) are determined. For example, to determine E_x a uniaxial tension test is assumed such that $\sigma_x \neq 0$ and $\sigma_y = \sigma_z = \tau_{yz} = \tau_{xz} = \tau_{xy} = 0$. The system of equations as in Equation 13 can then be rewritten as:

$$C_{11}\varepsilon_x + C_{12}\varepsilon_y + C_{13}\varepsilon_z + C_{16}\gamma_{xy} = \sigma_x \tag{14}$$
$$C_{12}\varepsilon_x + C_{22}\varepsilon_y + C_{23}\varepsilon_z + C_{26}\gamma_{xy} = 0 \tag{15}$$
$$C_{13}\varepsilon_x + C_{23}\varepsilon_y + C_{33}\varepsilon_z + C_{36}\gamma_{xy} = 0 \tag{16}$$
$$C_{16}\varepsilon_x + C_{26}\varepsilon_y + C_{36}\varepsilon_z + C_{66}\gamma_{xy} = 0 \tag{17}$$

Rearranging Equations 15 - 17 gives:

$$\varepsilon_y = \frac{-C_{12}\varepsilon_x - C_{23}\varepsilon_z - C_{26}\gamma_{xy}}{C_{22}} \tag{18}$$
$$\varepsilon_z = \frac{-C_{13}\varepsilon_x - C_{23}\varepsilon_y - C_{36}\gamma_{xy}}{C_{33}} \tag{19}$$
$$\gamma_{xy} = \frac{-C_{16}\varepsilon_x - C_{26}\varepsilon_y - C_{36}\varepsilon_z}{C_{66}} \tag{20}$$

Inserting Equation 18 in Equation 19, regrouping, and simplifying gives:

$$\varepsilon_z = -\nu_{xz}\varepsilon_x \tag{21}$$

where,

$$\nu_{xz} = \frac{C_{13}C_{26}^2 - C_{16}C_{23}C_{26} - C_{12}C_{26}C_{36} + C_{16}C_{22}C_{36} + C_{12}C_{23}C_{66} - C_{13}C_{22}C_{66}}{C_{66}C_{23}^2 - 2C_{23}C_{26}C_{36} + C_{33}C_{26}^2 + C_{22}C_{36}^2 - C_{22}C_{33}C_{66}}$$

The same procedure is performed by inserting Equation 19 in Equation 18:

$$\varepsilon_y = -\nu_{xy}\varepsilon_x \tag{22}$$

where,

$$\nu_{xy} = \frac{C_{12}C_{36}^2 - C_{13}C_{26}C_{36} - C_{16}C_{23}C_{36} + C_{16}C_{26}C_{33} + C_{13}C_{23}C_{66} - C_{12}C_{33}C_{66}}{C_{66}C_{23}^2 - 2C_{23}C_{26}C_{36} + C_{33}C_{26}^2 + C_{22}C_{36}^2 - C_{22}C_{33}C_{66}}$$

Substituting Equations 21 and 22 into Equation 20 gives:

$$\gamma_{xy} = \frac{-C_{12} + C_{26}\nu_{xy} + C_{36}\nu_{xz}}{C_{66}}\varepsilon_x \tag{23}$$

Finally, insert Equations 21, 22, and 23 back into Equation 14 to give the expression for E_x:

$$\sigma_x = E_x \varepsilon_x$$

where,

$$E_x = C_{11} - \nu_{xy}\left(C_{12} - \frac{C_{16}C_{26}}{C_{66}}\right) - \nu_{xz}\left(C_{13} - \frac{C_{16}C_{36}}{C_{66}}\right) - \frac{C_{16}^2}{C_{66}} \tag{24}$$

In a similar fashion E_y and E_z and the corresponding Poisson's ratios can be derived:

$$E_y = C_{22} - \nu_{yx}\left(C_{12} - \frac{C_{16}C_{26}}{C_{66}}\right) - \nu_{yz}\left(C_{23} - \frac{C_{26}C_{36}}{C_{66}}\right) - \frac{C_{26}^2}{C_{66}} \tag{25}$$

where,

$$\nu_{yz} = \frac{C_{16}^2C_{23} - C_{13}C_{16}C_{26} - C_{12}C_{16}C_{36} + C_{11}C_{26}C_{36} + C_{12}C_{13}C_{66} - C_{11}C_{23}C_{66}}{C_{66}C_{13}^2 - 2C_{13}C_{16}C_{36} + C_{33}C_{16}^2 + C_{11}C_{36}^2 - C_{11}C_{33}C_{66}}$$

$$\nu_{yx} = \frac{C_{12}C_{36}^2 - C_{13}C_{26}C_{36} - C_{16}C_{23}C_{36} + C_{16}C_{26}C_{33} + C_{13}C_{23}C_{66} - C_{12}C_{33}C_{66}}{C_{66}C_{13}^2 - 2C_{13}C_{16}C_{36} + C_{33}C_{16}^2 + C_{11}C_{36}^2 - C_{11}C_{33}C_{66}}$$

and,

$$E_z = C_{33} - \nu_{zx}\left(C_{13} - \frac{C_{16}C_{36}}{C_{66}}\right) - \nu_{zy}\left(C_{23} - \frac{C_{26}C_{36}}{C_{66}}\right) - \frac{C_{36}^2}{C_{66}} \tag{26}$$

where,

$$\nu_{zy} = \frac{C_{16}^2C_{23} - C_{13}C_{16}C_{26} - C_{12}C_{16}C_{36} + C_{11}C_{26}C_{36} + C_{12}C_{13}C_{66} - C_{11}C_{23}C_{66}}{C_{66}C_{12}^2 - 2C_{12}C_{16}C_{26} + C_{22}C_{16}^2 + C_{11}C_{26}^2 - C_{11}C_{22}C_{66}}$$

$$\nu_{zx} = \frac{C_{13}C_{26}^2 - C_{16}C_{23}C_{26} - C_{12}C_{26}C_{36} + C_{16}C_{22}C_{36} + C_{12}C_{23}C_{66} - C_{13}C_{22}C_{66}}{C_{66}C_{12}^2 - 2C_{12}C_{16}C_{26} + C_{22}C_{16}^2 + C_{11}C_{26}^2 - C_{11}C_{22}C_{66}}$$

For determining G_{yz} it is assumed that $\tau_{yz} \neq 0$ and $\sigma_x = \sigma_y = \sigma_z = \tau_{xz} = \tau_{xy} = 0$. The system of equations as in Equation 13 are then rewritten as:

$$C_{44}\gamma_{yz} + C_{45}\gamma_{xz} = \tau_{yz} \tag{27}$$

$$C_{45}\gamma_{yz} + C_{55}\gamma_{xz} = 0 \tag{28}$$

Rewriting Equation 28 and substituting in Equation 27 gives:

$$\tau_{yz} = G_{yz}\gamma_{yz}$$

where,

$$G_{yz} = C_{44} - \frac{C_{45}^2}{C_{55}} \tag{29}$$

Similarly for G_{xz} this gives:

$$G_{xz} = C_{55} - \frac{C_{45}^2}{C_{44}} \tag{30}$$

The derivation of G_{xy} is performed similarly to the derivation of E_x which results in:

$$G_{xy} = C_{66} - \nu_{xyy}\left(C_{26} - \frac{C_{12}C_{16}}{C_{11}}\right) - \nu_{xyz}\left(C_{36} - \frac{C_{13}C_{16}}{C_{11}}\right) - \frac{C_{16}^2}{C_{11}} \tag{31}$$

where,

$$\nu_{xyz} = \frac{C_{12}^2C_{36} - C_{12}C_{13}C_{26} - C_{12}C_{16}C_{23} + C_{13}C_{16}C_{22} + C_{11}C_{23}C_{26} - C_{11}C_{22}C_{36}}{C_{33}C_{12}^2 - 2C_{12}C_{13}C_{23} + C_{22}C_{13}^2 + C_{11}C_{23}^2 - C_{11}C_{22}C_{33}}$$

$$\nu_{xyy} = \frac{C_{13}^2C_{26} - C_{13}C_{16}C_{23} - C_{12}C_{13}C_{36} + C_{12}C_{16}C_{33} + C_{11}C_{23}C_{36} - C_{11}C_{26}C_{33}}{C_{33}C_{12}^2 - 2C_{12}C_{13}C_{23} + C_{22}C_{13}^2 + C_{11}C_{23}^2 - C_{11}C_{22}C_{33}}$$

References

1. Richardson MOW and Wisheart MJ. Review of low-velocity impact properties of composite materials. *Composites Part A: Applied Science and Manufacturing* 1996; 27(12): 1123–1131. DOI:10.1016/1359-835X(96)00074-7.
2. Davies GAO and Olsson R. Impact on composite structures. *The Aeronautical Journal* 2004; 108: 541–563. DOI: 10.1017/S0001924000000385.
3. Abrate S. Modeling of impacts on composite structures. *Composite Structures* 2001; 51(2): 129–138.
4. Agrawal S, Singh KK and Sarkar PK. Impact damage on fibre-reinforced polymer matrix composite - a review. *Journal of Composite Materials* 2019; 48(3): 317–332. DOI:10.1177/0021998312472217.
5. Shivakumar KN, Elber W and Illg W. Prediction of impact force and duration due to low-velocity impact on circular composite laminates. *Journal of Applied Mechanics* 1985; 52(3): 674–680. DOI:10.1115/1.3169120.
6. Olsson R. Impact response of orthotropic composite plates predicted from a one-parameter differential equation. *AIAA Journal* 1992; 30(6): 1587–1596. DOI:10.2514/3.11105.
7. Olsson R. Mass criterion for wave controlled impact response of composite plates. *Composites Part A: Applied Science and Manufacturing* 2000; 31(8): 879–887. DOI:10.1016/S1359-835X(00)00020-8.
8. Olsson R. Analytical prediction of large mass impact damage in composite laminates. *Composites: Part A* 2001; 32: 1207–1215. DOI:10.1016/S1359-835X(01)00073-2.
9. Olsson R. Analytical model for delamination growth during small mass impact. *International Journal of Solids and Structures* 2010; 47: 2884–2892. DOI:10.1016/j.ijsolstr.2010.06.015.
10. Christoforou AP and Swanson SR. Analysis of impact response in composite plates. *International Journal of Solids and Structures* 1991; 27(2): 161–170. DOI:10.1016/0020-7683(91)90226-6.
11. Christoforou AP and Yigit AS. Characterization of impact in composite plates. *Composite Structures* 1998; 43: 14–24. DOI:10.1016/S0263-8223(98)00087-7.
12. Talagani MR. *Impact analysis of composite structures*. Phd thesis, Delft University of Technology, 2014. URL `http://resolver.tudelft.nl/uuid:f576163e-3d28-4b76-b50e-2431622c1da5`.
13. Esrail F and Kassapoglou C. An efficient approach for damage quantification in quasi-isotropic composite laminates under low speed impact. *Composites Part B: Engineering* 2014; 61: 116–126. DOI:10.1016/j.compositesb.2014.01.033.
14. Bouvet C, Rivallant S and Barrau JJ. Low velocity impact modeling in composite laminates capturing permanent indentation. *Composites Science and Technology* 2012; 72(16): 1977–1988. DOI:10.1016/j.compscitech.2012.08.019.
15. Rivallant S, Bouvet C and Hongkarnjanakul N. Failure analysis of CFRP laminates subjected to compression after impact: FE simulation using discrete interface elements. *Composites Part A: Applied Science and Manufacturing* 2013; 55: 83–93. DOI:10.1016/j.compositesa.2013.08.003.

16. Hongkarnjanakul N, Bouvet C and Rivallant S. Validation of low velocity impact modelling on different stacking sequences of CFRP laminates and influence of fibre failure. *Composite Structures* 2013; 106: 549 – 559. DOI: 10.1016/j.compstruct.2013.07.008.
17. Tan W, Falzon BG, Chiu LNS et al. Predicting low velocity impact damage and Compression-After-Impact (CAI) behaviour of composite laminates. *Composites Part A: Applied Science and Manufacturing* 2015; 71: 212–226. DOI:10.1016/j.compositesa.2015.01.025.
18. Mittal RK. A simplified analysis of the effect of transverse shear on the response of elastic plates to impact loading. *International Journal of Solids and Structures* 1987; 23(8): 1191 – 1203. DOI:10.1016/0020-7683(87)90055-2.
19. Sun CT and Potti SV. A simple model to predict residual velocities of thick composite laminates subjected to high velocity impact. *International Journal of Impact Engineering* 1996; 18(3): 339–353. DOI:10.1016/0734-743X(96)89053-1.
20. Potti SV and Sun CT. Prediction of impact induced penetration and delamination in thick composite laminates. *International Journal of Impact Engineering* 1997; 19(1): 31–48. DOI:10.1016/S0734-743X(96)00005-X.
21. Zhou G and Davies GA. Impact response of thick glass fibre reinforced polyester laminates. *International Journal of Impact Engineering* 1995; 16(3): 357–374. DOI:10.1016/0734-743X(94)00047-Z.
22. Jackson WC and Poe Jr CC. The use of impact force as a scale parameter for the impact response of composite laminates. *Journal of Composites, Technology and Research* 1993; 15(4): 282–289. DOI:10.1520/CTR10380J.
23. van Hoorn N, Kassapoglou C and van den Brink WM. Impact response of thick composite structures. techreport NLR-TP-2017-460, NLR - Netherlands Aerospace Centre, 2017.
24. van Hoorn N, Kassapoglou C and van den Brink WM. Impact response of thick composite structures. In Remmers JJC and Turon A (eds.) *6th ECCOMAS Thematic Conference on the Mechanical Response of Composites*. Eindhoven University of Technology.
25. Hertz H and Lenard PEA. *Gesammelte werke*. Leipzig: Barth, J. A., 1895.
26. Christoforou AP and Yigit AS. Transient response of a composite beam subject to elasto-plastic impact. *Composites Engineering* 1995; 5(5): 459–470. DOI:10.1016/0961-9526(95)00018-I.
27. Yang SH and Sun CT. Indentation law and for composite and laminates. In Daniel I (ed.) *Composite Materials: Testing and Design (6th Conference)*. STP28494S, West Conshohocken, PA: ASTM International, pp. 425–449.
28. Whitney JM and Pagano NJ. Shear deformation in heterogeneous anisotropic plates. *Journal of Applied Mechanics* 1970; 37(4): 1031–1036. DOI:10.1115/1.3408654.
29. Dobyns AL. Analysis of simply-supported orthotropic plates subject to static and dynamic loads. *AIAA Journal* 1981; 19(5): 642–650. DOI:10.2514/3.50984.
30. Sun CT and Chen JK. On the impact of initially stressed composite laminates. *Journal of Composite Materials* 1985; 19(6): 490–504. DOI:10.1177/002199838501900601.
31. Soden PD, Hinton MJ and Kaddour AS. Lamina properties, lay-up configurations and loading conditions for a range of fibre-reinforced composite laminates. *Composites Science and Technology* 1998; 58(7): 1011–1022. DOI: 10.1016/S0266-3538(98)00078-5.
32. Hashin Z. Analysis of composite materials — a survey. *Journal of Applied Mechanics* 1983; 50(3): 481–505. DOI:10.1115/1.3167081.
33. Saltelli A, Annoni P, Azzini I et al. Variance based sensitivity analysis of model output. Design and estimator for the total sensitivity index. *Computer Physics Communications* 2010; 181(2): 259–270. DOI:10.1016/j.cpc.2009.09.018.
34. Sobol IM. Global sensitivity indices for nonlinear mathematical models and their Monte Carlo estimates. *Mathematics and Computers in Simulation* 2001; 55(1): 271–280. DOI:10.1016/S0378-4754(00)00270-6.
35. Kassapoglou C. *Design and analysis of composite structures*. John Wiley & Sons, Ltd, 2010. DOI:10.2514/4.867804.

Dedicated to innovation in aerospace

Royal Netherlands Aerospace Centre

NLR is a leading international research centre for aerospace. Bolstered by its multidisciplinary expertise and unrivalled research facilities, NLR provides innovative and integral solutions for the complex challenges in the aerospace sector.

NLR's activities span the full spectrum of Research Development Test & Evaluation (RDT & E). Given NLR's specialist knowledge and facilities, companies turn to NLR for validation, verification, qualification, simulation and evaluation. NLR thereby bridges the gap between research and practical applications, while working for both government and industry at home and abroad.

NLR stands for practical and innovative solutions, technical expertise and a long-term design vision. This allows NLR's cutting edge technology to find its way into successful aerospace programs of OEMs, including Airbus, Embraer and Pilatus. NLR contributes to (military) programs, such as ESA's IXV re-entry vehicle, the F-35, the Apache helicopter, and European programs, including SESAR and Clean Sky 2.

Founded in 1919, and employing some 600 people, NLR achieved a turnover of 76 million euros in 2017, of which 81% derived from contract research, and the remaining from government funds.

For more information visit: **www.nlr.org**

Postal address
PO Box 90502
1006 BM Amsterdam, The Netherlands
e) info@nlr.nl **i)** www.nlr.org

NLR Amsterdam
Anthony Fokkerweg 2
1059 CM Amsterdam, The Netherlands
p) +31 88 511 3113

NLR Marknesse
Voorsterweg 31
8316 PR Marknesse, The Netherlands
p) +31 88 511 4444